Combinatorial Screening of Polymer:Fullerene Blends for Organic Solar Cells by Inkjet Printing

*Anke Teichler, Rebecca Eckardt, Stephanie Hoeppener, Christian Friebe, Jolke Perelaer, Alessia Senes, Mauro Morana, Christoph J. Brabec, and Ulrich S. Schubert**

Polymer:fullerene blends were screened in a combinatorial approach using inkjet printing thin film libraries for photovoltaic devices. The application of inkjet printing enabled a fast and simple experimental workflow from film preparation to the study of structure-property-relationships with a very high material efficiency. Inkjet printing requires less material for the preparation of thin film libraries in comparison to other dispensing techniques, like spin-coating. Two polymers (PCPDTBT, PSBTBT) and two fullerene derivatives (mono-PCBM, bis-PCBM) were investigated in various blend ratios, concentrations, solvent ratios, and film thicknesses. Morphological and optical properties of the inkjet printed films were investigated and compared with spin-coated films. This study shows the principle of an experimental setup from solution preparation to film characterization for the combinatorial investigation of large polymer:fullerene libraries.

1. Introduction

Conjugated polymers are interesting candidates for optoelectronic devices due to their semi-conducting properties.[1] Moreover, conductive polymers show advanced processing properties, since they can be dissolved in a variety of organic solvents and, subsequently, can be processed into thin films. In recent research, conjugated polymers, such as poly(phenylene)s and polythiophenes, have been used in optoelectronic devices, including organic light-emitting diodes (OLEDs),[2,3] organic photovoltaics (OPVs),[4,5] and organic field-effect transistors (OFETs).[6,7] An important advantage of conjugated polymers is that the polymers can be tailored to optimize the final device properties, for example by adding side-chains to the polymer for an improved solubility or electron affinity.[8] The possibility of altering the material properties and the use of cheap processing methods, such as spin-coating or inkjet printing, classify conjugated polymers as promising materials for smaller, flexible, and, most importantly, cheaper devices for optoelectronic applications.[9,10]

Bulk heterojunction organic solar cells are interesting architectures that have been reported with high efficiencies.[1] This type of solar cell is based on a layered structure, where the active material consists of a mixture of donor and acceptor materials. Much research has been devoted in the last years to synthesize new polymer materials with a low bandgap.[11] In recent research, poly[2,6-(4,4-bis-(2-ethylhexyl)-4H-cyclopenta[2,1-b;3,4-b`]dithiophene)-*alt*-4,7(2,1,3-benzothiadiazole)] (PCPDTBT, **Figure 1**a) and poly[(4,4′-bis-(2-ethylhexyl)-dithieno(3,2-b;2′,3′-d)silole]-2,6-diyl-*alt*-(2,1,3-benzothiadiazole)-4,7-diyl] (PSBTBT) have been used as donor materials in bulk heterojunction solar cells (Figure 1b).[12] Although the chemical structure of PCPDTBT and PSBTBT is almost identical, apart from the bridging C-atom in the backbone that is replaced by a Si-atom, PSBTBT shows a higher crystallinity than PCPDTBT.[13,14] Power efficiencies in the range of 3.5% to 3.8% have been reported for PSBTBT and PCPDTBT solar cells.[13,15] Further increase of the power efficiency was obtained either by using an additive in the blend composition, resulting in efficiencies up to 5.5% for the polymer PCPDTBT,[16] or by a post-processing annealing step, whereby an efficiency of 5.6% was reported for PSBTBT.[13]

Frequently used acceptor materials are fullerene derivatives like mono(1-[3-(methoxycarbonyl)propyl]-1-phenyl)-[6,6]C_{61} (mono-PCBM, Figure 1c) and the higher substituted fullerene derivative bis(1-[3-(methoxycarbonyl)-propyl]-1-phenyl)-[6,6]C_{62} (bis-PCBM, Figure 1d) due to their high electron affinity. The latter fullerene compound shows a better solubility towards organic solvents than mono-PCBM and is therefore an interesting new candidate for solution deposition techniques. Furthermore, bis-PCBM shows a higher LUMO level, which

A. Teichler, R. Eckardt, Dr. S. Hoeppener, C. Friebe,
Dr. J. Perelaer, Prof. U. S. Schubert
Laboratory of Organic and Macromolecular Chemistry (IOMC)
Friedrich-Schiller-University, Jena
Humboldtstraße 10, 07743 Jena, Germany
E-mail: ulrich.schubert@uni-jena.de
A. Teichler, R. Eckardt, Dr. S. Hoeppener,
Dr. J. Perelaer, Prof. U. S. Schubert
Dutch Polymer Institute (DPI)
PO Box 902, 5600 AX Eindhoven, The Netherlands
A. Senes, Dr. M. Morana
Konarka Austria, Altenbergerstraße 69, 4040 Linz, Austria
Prof. C. J. Brabec
Institute of Material Science
Friedrich-Alexander-University Erlangen-Nürnberg
Martensstraße 7, 91058 Erlangen, Germany

DOI: 10.1002/aenm.201000027

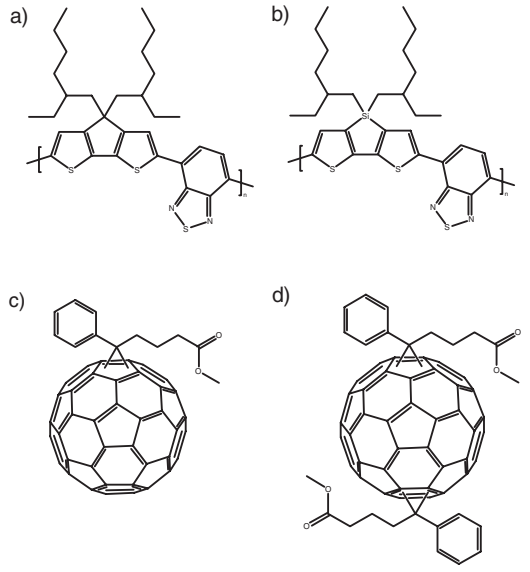

Figure 1. Schematic representation of the chemical structures of a) PCPDTBT, b) PSBTBT, c) mono-PCBM and d) bis-PCBM, respectively.

minimizes the energy loss during electron transfer from the donor to the acceptor material.[17]

The majority of the solar cell efficiencies reported in the open literature were obtained by spin-coating the active layer, whereas only a few reports on inkjet printing have been published.[18,19] Spin-coating is a fast and simple method to produce homogeneous thin films. However, a major drawback is that the majority of the material gets lost during processing, and, moreover, the application of a combinatorial workflow is not possible.[4,18] This represents a serious bottleneck, in particular for the development of new donor/acceptor materials for organic solar cells; the standard method does not allow a cheap approach to investigate new materials, since relatively large quantities are required. Inkjet printing is, indeed, a much more efficient tool in terms of handling materials. This solution deposition method is rapidly growing as a tool in scientific research on account of its low material waste production and on-demand as well as additive deposition of materials. Additionally, it is a non-contact and mask-less processing technique, showing clear advantages in comparison to other solution deposition methods, like spin-coating, doctor blading, and gravure printing.[20,21] Being a non-contact process, inkjet printing also enables large area and roll-to-roll (R2R) processing. Therefore, once a suitable candidate for preparing an organic solar cell has been found, inkjet printing is the right tool to prepare thin and homogeneous layers of the active materials. Hoth *et al.* showed that inkjet printing can be used for the preparation of solar cells by printing the active layer of poly(3-hexylthiophene) (P3HT) and 1-[3-(methoxycarbonyl)propyl]-1-phenyl)-[6,6]C_{61} (PCBM).[19,22,23]

However, a much more appealing approach would be to use inkjet printing for the preparation of thin-film libraries, which would subsequently allow a combinatorial workflow from film preparation to the elucidation of structure-property relationships.[24,25] By printing thin-film libraries, the influence of ink composition, substrate properties, and different printing parameters on the film properties can be studied in a fast, reproducible, and easy way with a maximum materials efficiency.[26,27] Critical parameters for the performance of bulk heterojunction solar cells are the donor/acceptor ratio, the film thickness, as well as the morphology of the resulting films. The optimal ratio between donor and acceptor material can be determined by fluorescence quenching and morphological investigations.[28,29] The morphology is very important for the efficiency of an organic solar cell since excitons have to reach a donor-acceptor interface within a few nanometers after being created; additionally, the created charges are required to reach the electrodes. Therefore, a good intermixing of donor and acceptor material is essential for a good device functionality. Beside the donor/acceptor ratio, the most important parameters that influence the nanoscale morphology are the processing solvent, the solute concentration, and the method of film preparation.[30–32] Inkjet printing of thin-film libraries allows a reproducible method for comparing different concentrations, ratios, and film thicknesses.[26]

Newly discovered donor/acceptor materials require a large number of combinations to be tested for their behavior in bulk heterojunction solar cell applications. Additionally, the parameters for film preparation have a significant influence on the properties of the active layer.[33,34] Therefore, an enormous number of samples need to be screened for the evaluation of promising polymer:fullerene combinations and good processing conditions. Instead of studying the potential materials in a sequential, one-by-one manner, for example by spin-coating, inkjet printing of thin-film libraries allows a fast screening of many materials in parallel. Thus, hundreds or even thousands of compounds may be investigated, which allows a significant speed-up of the research as well as a decrease in the research costs.

In this contribution, we present an experimental setup that allows the handling of a large number of samples and, subsequently, a combinatorial and reproducible screening of polymer:fullerene blends used for organic solar cells. This is realized by inkjet printing thin-film libraries with a systematically varied film thickness, concentration, solvent ratio, and blend composition, resulting in a minimal material consumption. The resulting inkjet printed films are screened for their morphological and optical properties, and subsequently compared to spin-coated films. Finally, two polymer:fullerene blend compositions are selected from the combinatorial study and tested for their solar cell activity.

2. Results and Discussion

2.1. Experimental Setup

The experimental workflow for the combinatorial screening of polymer:fullerene blends is shown in **Figure 2**. Using a pipetting robot, donor/acceptor solutions were prepared in a standard 96-well plate with a systematically varied compound ratio, solvent mixture, and concentration. The freshly prepared solutions in the well plate were used as small reservoirs with ink for the inkjet printing process. With a micropipette the inks

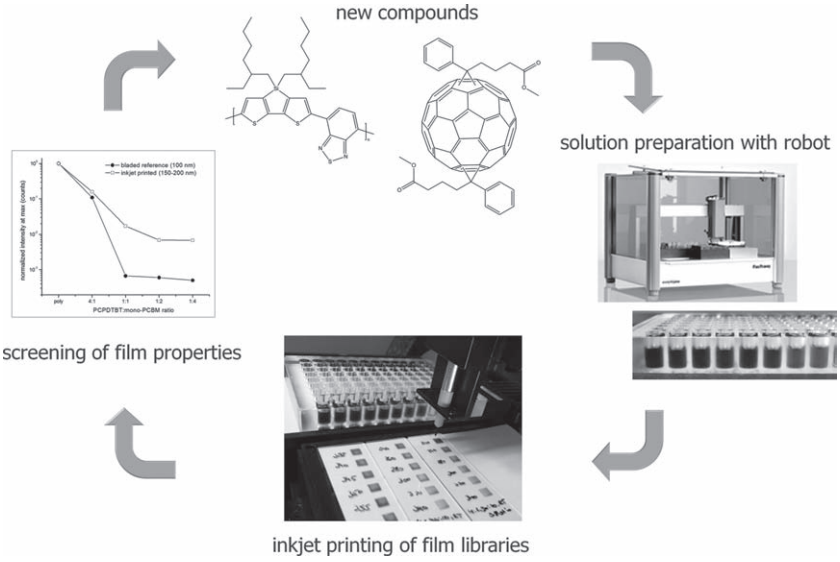

Figure 2. Experimental workflow for the combinatorial screening of donor/acceptor combinations for the use in organic solar cells.

were one-by-one aspirated from individual wells and printed on a substrate that is located on a heatable table. During printing the inks in the plate were stirred to keep the formulations homogeneous. The printing conditions that influence film thickness and homogeneity, for example dot spacing and substrate temperature, can easily be changed in the printer software. The thin-film libraries were printed onto the substrate in a microtiter plate layout, *i.e.* each film measures 5 mm × 5 mm and the distance of the rectangles corresponds to the distance between the wells in the plate. Such printed glass samples can serve perfectly as easily characterizable libraries for analytical tools, including UV-vis and FTIR spectroscopy, and RAMAN plate readers.

2.2. Spin-Coating

Spin-coating was used to prepare thin films of different polymer:fullerene blends. Although this method has been described extensively in literature, we use it here as a reference for the films that are prepared by inkjet printing, as described in the next section.

First, a single solvent (chlorobenzene, CB) was used for film preparation, which resulted in thin homogeneous films when using spin-coating, but not when using inkjet printing; all solute material was located at the perimeter of the as-printed film – an effect known as the "coffee ring" effect.[35] Inkjet printing from a solvent mixture has been reported to improve the film formation and can result in homogenous films.[26] Here, a solvent mixture of chlorobenzene and *ortho*-dichlorobenzene (*o*-DCB) was used, where the latter component was added in an amount of either 10% or 20% by volume. For a better comparison of spin-coated and inkjet printed films, spin-coating was performed using this solvent mixture. The solvent combination did not negatively influence the formation of spin-coated films.

The preferred film thickness for the active layer in a bulk heterojunction solar cell is between 100 and 200 nm.[30] We found that the spin-coating of PCPDTBT:mono-PCBM blends in the ratios from 4:1 to 1:4 with a concentration of 0.8 wt% leads to homogeneous films with thicknesses between 140 and 260 nm, which is above the desired thickness for blends with a higher fullerene content. Decreasing the concentration to 0.6 wt% resulted in film heights of between 130 and 150 nm for all blend ratios (**Table 1**). For PCPDTBT:mono-PCBM, a ratio of 1:3.4 is known to be the optimal ratio for balanced charge

Table 1. Film thicknesses and rms-values for inkjet printed and spin-coated films for PCPDTBT:bis-PCBM, PCPDTBT:mono-PCBM and PSBTBT:mono-PCBM prepared from different blend ratios and concentrations. The solvent ratio CB/*o*-DCB is 90/10.

		PCPDTBT:bis-PCBM			PCPDTBT:mono-PCBM			PSBTBT:mono-PCBM		
	wt%	ratio	film thickness (nm)	rms (nm)	ratio	film thickness (nm)	rms (nm)	ratio	film thickness (nm)	rms (nm)
Spin-coating	0.6	–	–	–	4:1	129	2	4:1	126	2
		–	–	–	1:1	139	1	1:1	130	2
		–	–	–	1:3.4	146	1	1:2	138	4
Inkjet printing	0.8	4:1	350	3	4:1	240	1	–	–	–
		1:1	340	2	1:1	280	1	–	–	–
		1:4	740	1	1:4	420	1	–	–	–
Inkjet printing	0.6	4:1	160	3	4:1	130	2	4:1	192	2
		1:3.4	230	1	1:1	190	1	1:1	245	3
		–	–	–	1:3.4	240	1	1:2	260	4
Inkjet printing	0.5	4:1	130	4	4:1	127	3	4:1	169	3
		1:3.4	170	1	1:1	142	1	1:1	178	15
		–	–	–	1:3:4	169	1	1:2	190	7

transport in the polymer solar cell.[29] Figure S1a (Supporting Information) depicts a 3D optical profiler and an atomic force microscopy (AFM) image of the blend ratio PCPDTBT:mono-PCBM 1:3.4 showing a homogeneous film with a root mean square (rms) roughness of only 1 to 2 nm. Also the other PCPDTBT:mono-PCBM blend ratios 4:1 and 1:1 revealed very smooth films (Table 1).

Spin-coating of the PSBTBT:mono-PCBM blends with ratios between 4:1 and 1:2 and a concentration of 0.6 wt% also gave homogeneous films with a thickness between 120 and 140 nm, respectively (Table 1). Optical profiler and AFM images show rms-roughnesses of 4 nm with an apparent formation of aggregates in the film (Figure S1b (Supporting Information)).

Despite obtaining homogeneous and smooth films by spin-coating, a disadvantage of this technique is its inefficient materials usage (>99% of the applied material is wasted). Moreover, the preparation of compound libraries is complicated and requires many samples that are processed individually. By switching to inkjet printing, however, only small quantities of solutions are required to fabricate thin and homogeneous films, since materials are placed on-demand and on user-defined locations. After printing unused material is transferred from the micropipette back into the corresponding well in the microtiter plate, hence, converting a >99% waste generation for spin-coating into a >90% yield for inkjet printing. Furthermore with inkjet printing, thin-film libraries can be created and characterized in a combinatorial approach, revealing important structure-property relationships. Less material is required while the reproducibility as well as the reliability of the measurements increases. However, suitable inks have to be developed and optimized for their drying behavior, *i.e.* to prevent the coffee ring effect, as mentioned earlier.

2.3. Inkjet Printing

Inkjet printing was used for the investigation of three different polymer:fullerene blends; PCPDTBT:bis-PCBM, PCPDTBT:mono-PCBM, and PSBTBT:mono-PCBM.

First, the PCPDTBT:bis-PCBM blend was used to investigate the influence of the ratio between CB and *o*-DCB. The ratios 90/10 and 80/20 were chosen, whereby the minor part of the solvent mixture represents the higher boiling *o*-DCB. Subsequently, the PCPDTBT:bis-PCBM blends were inkjet printed using three different solute ratios (4:1, 1:1, and 1:4) and a concentration of 0.8 wt%. **Figure 3**a shows, from left to right, topographical images of printed films for the solvent ratio 90/10 and the three different blend ratios 4:1, 1:1, and 1:4, respectively. A good film formation was obtained with a PCPDTBT:bis-PCBM ratio of 4:1 and 1:1, while a higher fullerene content in the blend ratio (1:4) leads to less homogeneous films. This may be explained by the increased total concentration of the solute material with an increased amount of bis-PCBM.

When changing the solvent ratio to 80/20, homogeneous films were obtained solely when printed in a blend ratio of 4:1, while other blend ratios revealed less homogeneous films (Figure 3b). Therefore, it can be concluded that the solvent system CB/*o*-DCB with a ratio of 90/10 is more suitable for printing than 80/20. This may be explained by the longer drying time of the solvent ratio 80/20. It was recently reported that the time of solvent evaporation and the time of solute diffusion play a crucial role in the "coffee ring" effect.[36]

Morphological investigations by AFM revealed a good intermixing of the polymer and fullerene components for all PCPDTBT:bis-PCBM films obtained from both solvent systems, as depicted in Figure 3c and d. It can be seen that the rms-roughness for the solvent ratio 90/10 (Figure 3c) decreased with an increased fullerene content, while for the solvent ratio 80/20 (Figure 3d) no trend in the roughness could be observed. Based on the fact that the morphological images show a better film formation for the solvent system 90/10, this particular solvent mixture was chosen for all further inkjet printing experiments.

Table 1 summarizes the film thicknesses for films printed with the solvent ratio 90/10 and a concentration of 0.8 wt%. The blend ratios 4:1 and 1:1 resulted in a film thickness of approximately 350 nm, while a ratio of 1:4 led to films with a thickness of 740 nm. An increased film thickness is to be expected when the fullerene content increases due to an increase in the total solute concentration, whereas the polymer concentration is kept constant at 0.8 wt%. Equal thicknesses for the blends 4:1 and 1:1 resulted from the different dot spacings that were found to result in the most homogeneous films.

As mentioned before, the optimal thickness of the active layer in a bulk heterojunction solar cell is between 100 and 200 nm, which excludes using a concentration of 0.8 wt%. A sufficiently low film thickness for all blend ratios was only observed for a concentration of 0.5 wt%, whereas a concentration of 0.6 wt% only led to a film thickness below 200 nm for low fullerene content in the blend (Table 1). The UV-vis absorption spectra of the inkjet printed PCPDTBT:bis-PCBM blends are shown in Figure S3a (Supporting Information) for all three concentrations.

The second investigated blend system was PCPDTBT:mono-PCBM. Using this system with a concentration of 0.5 wt%, film thicknesses between 130 and 170 nm were reached, when printed from the solvent CB/*o*-DCB in a ratio 90/10. **Figure 4**a shows the homogeneous film formation for the blend ratios 4:1, 1:1, and 1:3.4, and a concentration of 0.5 wt%. Corresponding AFM images of the blends (Figure 4b) indicate a good intermixing of the blend compounds at all solute ratios. Aggregate formation was only observed in the blend ratio 4:1, whereas a smoother surface was found for the blend ratios 1:1 and 1:3.4 as confirmed by the decreased rms-roughness. Table 1 shows that the concentrations 0.8 wt% and 0.6 wt% are too high to obtain a film thickness below 200 nm at all ratios (see also Figure S4 (Supporting Information)).

UV-vis absorption spectra of spin-coated and inkjet printed films for the three blend ratios 4:1, 1:1 and 1:3.4 are depicted in **Figure 5**. The absorption spectra of spin-coated (Figure 5a) and inkjet printed films (Figure 5b: 0.6 wt%, Figure 5c: 0.5 wt%) show a superposition of the absorption of the two blend compounds. The absorption peak of mono-PCBM at 340 nm increases in intensity with increased fullerene content in the blends 1:1 and 1:3.4. The absorption of the polymer PCPDTBT shows a maximum at 765 nm and a peak with a lower intensity at 410 nm. Spin-coated films reveal a slightly red-shifted absorption compared to the corresponding inkjet printed films. The absorption maximum of the polymer at 765 nm is shifted to shorter wavelengths with higher mono-PCBM content in the

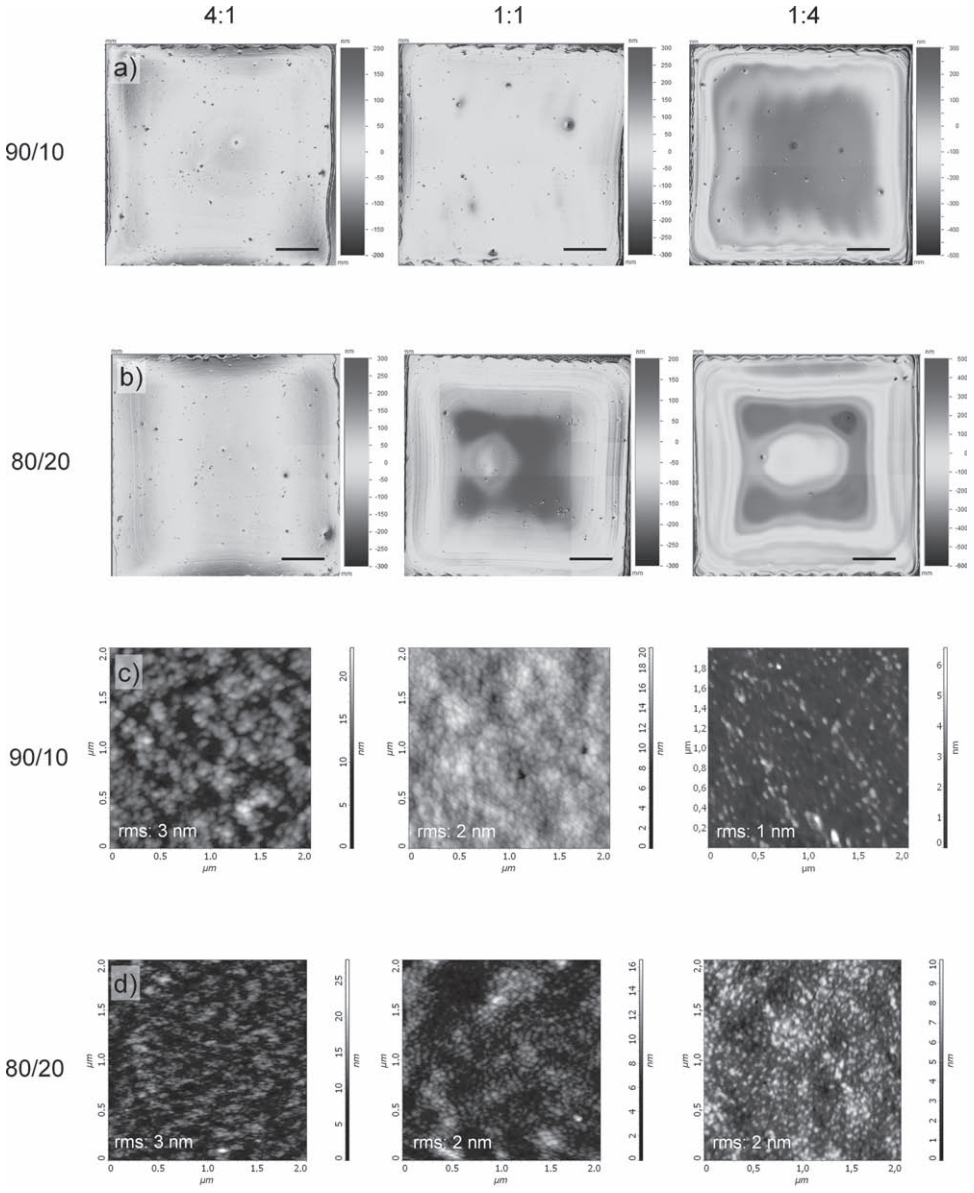

Figure 3. Optical profiler (a,b) and AFM (c,d) images of PCPDTBT:bis-PCBM films in a ratio, from left to right, of 4:1, 1:1, and 1:4, respectively. The films were inkjet printed from CB/*o*-DCB with a ratio of 90/10 (a, c) and 80/20 (b, d), while the concentration was 0.8 wt%. The black scale bars correspond to 1 mm. In white are the rms values for the film roughness.

blend for spin-coated films. For inkjet printed films using a concentration of 0.6 wt% the absorption maximum of the polymer at 765 nm remains at the same position, but the shoulder at 700 nm is slightly broadened with decreased fullerene content. In comparison, inkjet printing from a concentration of 0.5 wt% leads to a slight blue shift.

The quenching of fluorescence of the donor/acceptor ratios is an important hint for an efficient donor/acceptor combination. Photoluminescence measurements on the inkjet printed films from PCPDTBT:mono-PCBM showed a significant quenching to approximately 1% of the pure polymer emission intensity upon increased fullerene content in the blend (see **Figure 6**). This confirms the intermixing of the two blend components and an efficient charge transfer from the electron-donator PCPDTBT to the electron-acceptor mono-PCBM.

The third investigated blend system consisted of PSBTBT and mono-PCBM with ratios that were systematically varied from 4:1 to 1:2. The solubility of the polymer PSBTBT in CB/*o*-DCB is reduced due to its crystalline behavior when compared to the analogue PCPDTBT. Therefore, inkjet printing was less trivial than printing blends with PCPDTBT. We observed the formation of agglomerates in the films that may depend on the shelf-lifetime of the blend solutions. After preparing the inks, the solutions were handled at room temperature without further stirring; the best film formation was observed when printing directly after ink preparation.

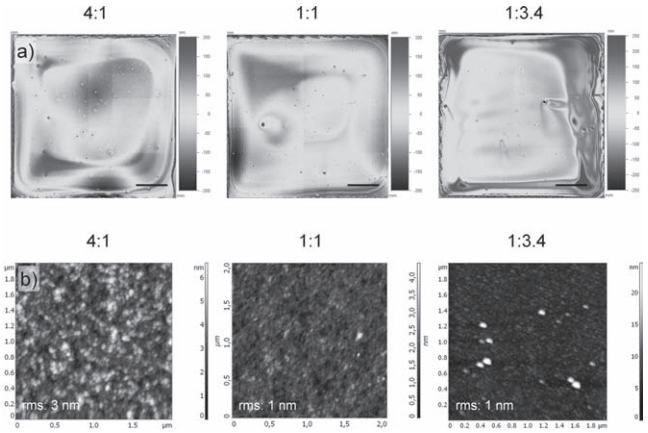

Figure 4. Optical profiler images (a) and AFM images (b) of PCPDTBT:mono-PCBM films in a ratio, from left to right, of 4:1, 1:1 and 1:3.4, respectively. The films were inkjet printed from CB/*o*-DCB with a ratio of 90/10, while the concentration was 0.5 wt%. The black scale bars (a) correspond to 1 mm and in white (b) are the rms values for the film roughness.

Inkjet printed thin-film libraries of PSBTBT:mono-PCBM, prepared from the solvent system CB/*o*-DCB 90/10 and a concentration of 0.5 wt%, are shown in Figure S5 (Supporting Information). Optical profiler images in Figure S5a (Supporting Information) revealed the formation of agglomerates. All films showed an increased roughness compared to PCPDTBT:mono-PCBM films, Figure S5b (Supporting Information), indicated by the higher rms roughness values. Only a blend ratio PSBTBT:mono-PCBM of 4:1 forms a smooth film with a roughness of 3 nm, while increased fullerene content increases the roughness (Table 1). Film thicknesses between 170 and 190 nm were obtained for all ratios and a concentration of 0.5 wt%, while a concentration of 0.6 wt% leads to a film thickness higher than 200 nm for all ratios (see also Figure S6 (Supporting Information)). Although, according to the optical images in Figure S5 (Supporting Information), the resulting films for a ratio of 1:1 may look more continuous, a larger fullerene content (ratio 1:2) revealed a lower roughness in comparison to the ratio 1:1. As a consequence, a concentration of 0.5 wt% and a blend ratio of 1:2 were chosen for the solar cell studies.

The different film forming properties of the blends PCPDTBT:mono-PCBM and PSBTBT:mono-PCBM can be explained by their difference in crystallinity.[13,14] Furthermore, the small changes in the chemical structure of the two polymers also caused significant changes in the UV-vis absorption spectra (**Figure 7**). The crystallinity of PSBTBT:mono-PCBM can be observed for all ratios by the double peaks in the region between 650 and 800 nm. The blends show an absorption maximum of the polymer at 765 nm with a shoulder around 700 nm and a third peak at 420 nm. With increased fullerene content, the corresponding absorption peak at 340 nm becomes more dominant, similar to the PCPDTBT:mono-PCBM blend system. Spin-coated films show a blue-shifted absorption (Figure 7a) in comparison to the corresponding inkjet printed films (Figure 7b). With increased fullerene content in the blend, the absorption maximum of PSBTBT is slightly red-shifted for both film preparation techniques. The absorption

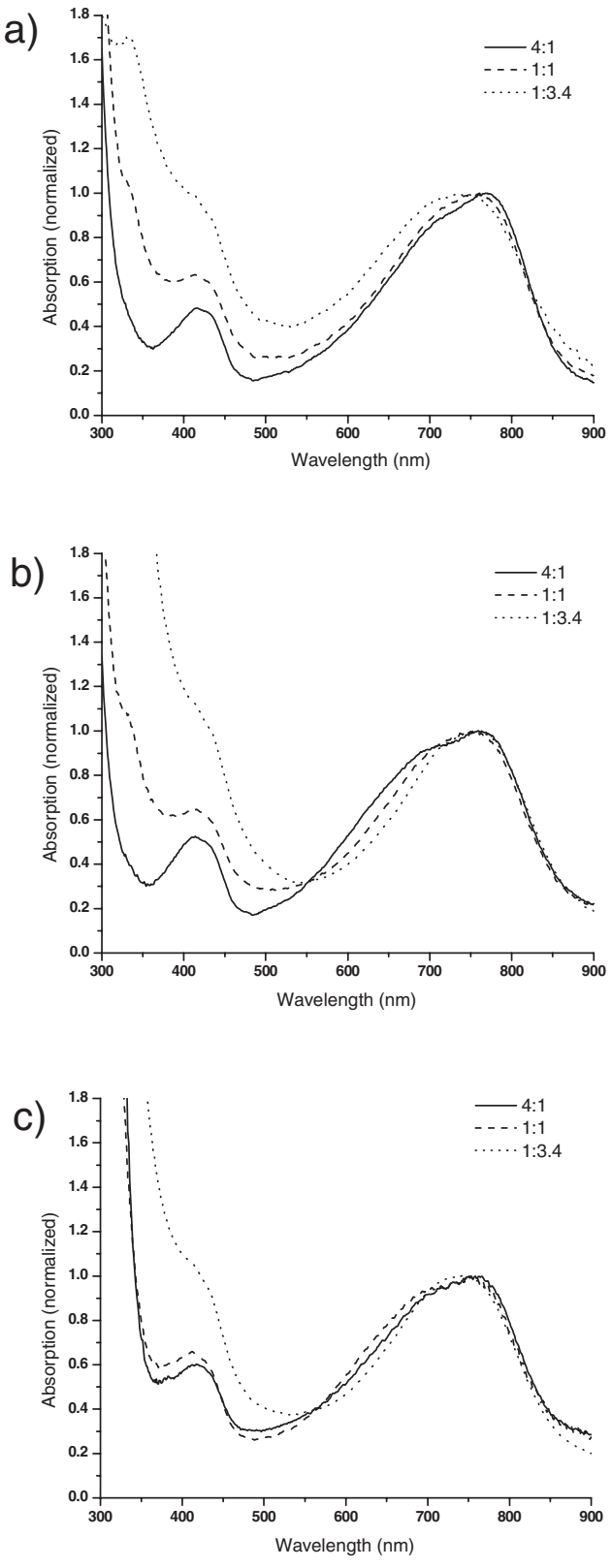

Figure 5. Normalized UV-vis absorption spectra of PCPDTBT:mono-PCBM 4:1, 1:1 and 1:3.4, prepared by spin-coating (a) and inkjet printing (b) from CB/*o*-DCB 90/10 with a concentration of 0.6 wt% and prepared by inkjet printing from a concentration of 0.5 wt% (c).

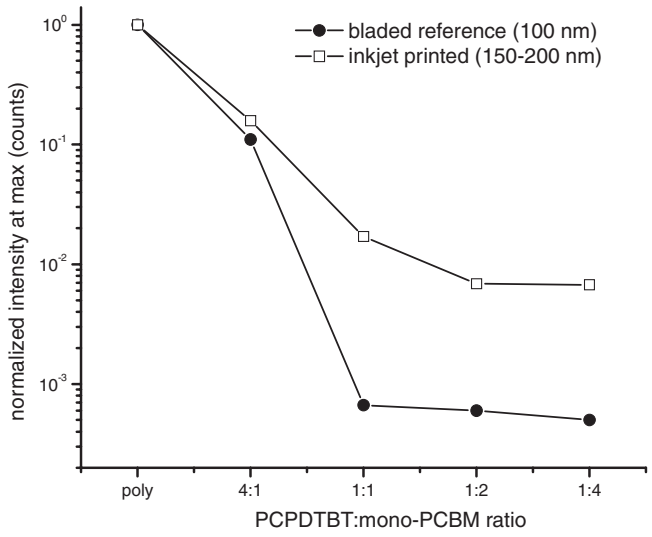

Figure 6. Normalized photoluminescent signal at maximum of PCPDTBT:mono-PCBM films prepared by inkjet printing (open squares) and by blading (closed circles) with varied ratios.

peak at 700 nm shows a decreased intensity with increased fullerene content for inkjet printed films for a concentration of 0.6 wt%, *i.e.* the polymer absorption is affected by the fullerene addition, which can be related to a decreased homogeneity upon increased fullerene concentration. In contrast, for inkjet printed films prepared from a concentration of 0.5 wt% and spin-coated films (0.6 wt%) the intensity of this peak increases with a PSBTBT:mono-PCBM ratio of 1:2.

The high crystallinity and thereby the reduced solubility of the polymer PSBTBT in organic solvents may become a drawback for long-term inkjet printing processes. A fast ink preparation and processing shows reproducible results; for the preparation of larger libraries, however, solubility issues become more pronounced. Therefore, initial tests to inkjet print the blend PSBTBT:mono-PCBM at elevated temperatures have been performed. A heatable dispenser nozzle (AD-K-801) was used that is able to heat the solution, tubing and nozzle tip up to 100 °C. **Figure 8**a shows 3D optical profiler images of PSBTBT:mono-PCBM (ratio 1:2) films printed at room temperature and from the heated solution (60 °C). A clear improvement in film formation can be observed when printing from the heated solution, since the formation of agglomerates is significantly reduced. Corresponding AFM images (Figure 8b) of the films show a similar rms roughness as printed at room temperature, as well as a comparable film morphology.

The heatable dispenser nozzle enables printing at elevated temperatures, but performing a combinatorial study analogous to the work undertaken with the micropipette nozzle is not possible due to a fundamental difference between the dispenser and micropipette nozzle. Namely, the micropipette aspirates small quantities of liquid up to 25 µL, while the dispenser head is supplied by a comparatively large built-in reservoir, holding up to 4 mL. In the case of the micropipette, the ink can be replaced quickly and in an automated fashion by programming a sequence of simple purging and aspirating steps; in contrast, a dispenser head requires first dismounting the reservoir

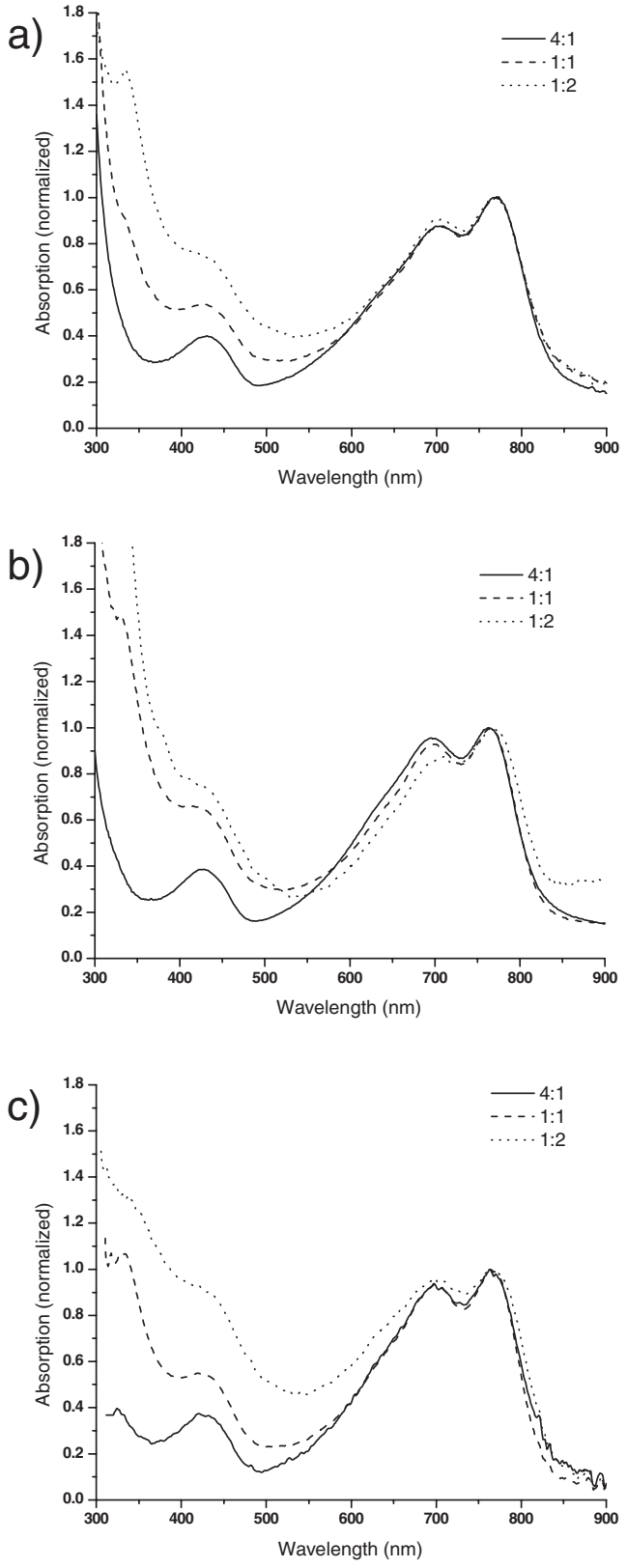

Figure 7. Normalized UV-vis absorption spectra of PSBTBT:mono-PCBM 4:1, 1:1 and 1:2, prepared by spin-coating (a) and inkjet printing (b) from CB/*o*-DCB 90/10 with a concentration of 0.6 wt% and prepared by inkjet printing from a concentration of 0.5 wt% (c).

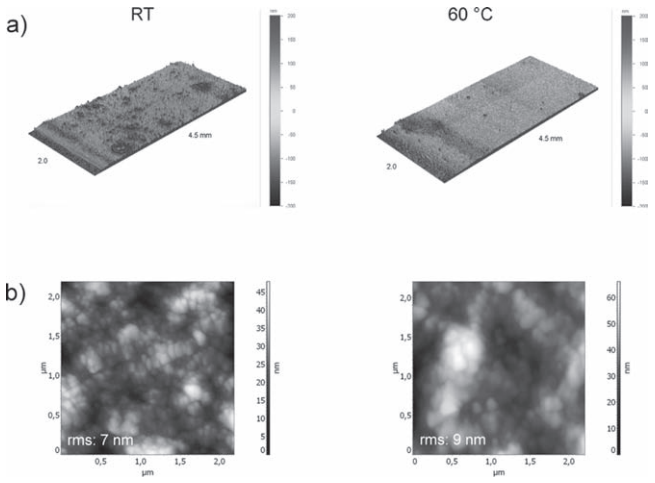

Figure 8. 3D optical profiler (a) and AFM (b) images of PSBTBT:mono-PCBM films in a ratio of 1:2. The films were inkjet printed from CB/*o*-DCB with a ratio of 90/10, while the concentration was 0.5 wt%, at room temperature and at 60 °C. In white (b) are the rms values for the film roughness.

hardware, followed by a cleaning step by flushing with a solvent and finally a refill of another ink. Moreover, larger volumes of ink would be necessary when printing from a dispenser nozzle.

2.4. Performance of Test Organic Solar Cells

From the optimization study, the systems PCPDTBT:mono-PCBM (ratio 1:3.4) and PSBTBT:mono-PCBM (ratio 1:2) were selected as candidates to prepare organic solar cells. A detailed description of the solar cells can be found in the experimental details.

Figure 9 shows *J-V* curves of the fabricated solar cells of the two polymer:fullerene systems. Some variation was observed upon photovoltaic parameters extraction from the *J-V* curves that may be assigned to a locally low homogeneity and a large film roughness in particular at the edges of the film. The photovoltaic parameters are summarized in **Table 2**. In the case of the PCPDTBT:mono-PCBM blend (Figure 9a), a rather ideal *J-V* characteristic could be observed with optimal open circuit voltage (V_{oc}), but affected by a rather low photocurrent at short circuit and very low fill factor (FF) compared to other devices that have been reported in literature.[12,14,15] The good rectification and the overlap of the injection current in dark and under illumination allows excluding the presence of significant shunts or series resistance limitations. The reason behind the non-optimal photogeneration and transport reducing the short circuit current density (J_{sc}) and FF may therefore be attributed to a non-optimal blend morphology.

For the PSBTBT:mono-PCBM system (Figure 9b), a similar behavior was observed with respect to current photogeneration issues. Two important differences, however, appear in the FF and in the forward injection regime. As illustrated in Figure 9c, the *J-V* curve of PSBTBT devices is affected by a kink for applied voltages approaching V_{oc}. The kink strongly reduces the FF. Furthermore, by analyzing the current at positive applied

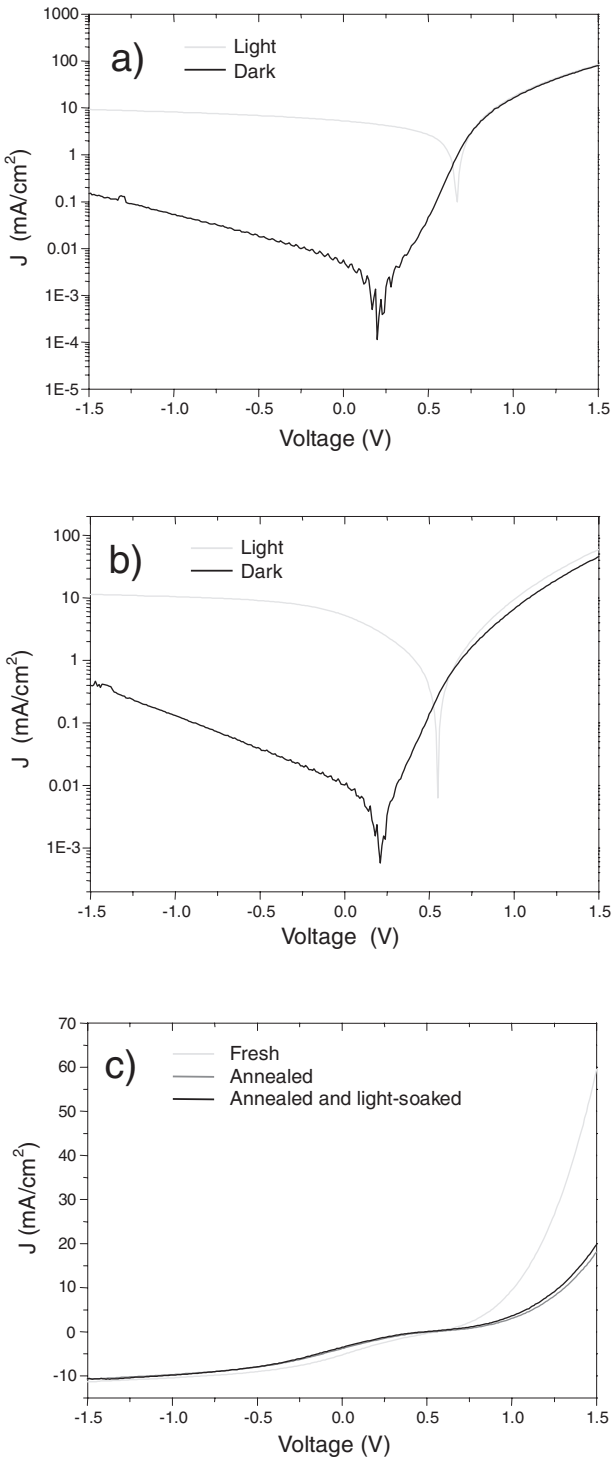

Figure 9. *J-V* characteristics of solar cells prepared from inkjet printed PCPDTBT:mono-PCBM (1:3.4) (a) and PSBTBT:mono-PCBM (1:2) (b) films with measurements under light/dark conditions. PSBTBT:mono-PCBM film (c) measured under simulated AM1.5 conditions and in linear representation.

voltages beyond V_{oc}, it can be seen that the previous effect also slightly reduces the forward current injection compared to the carbon-bridged analogue. The origin of the kink is not clear, but

Table 2. Photovoltaic parameters of the best devices selected from the inkjet printed plates.

	J_{sc}(mA/cm^2)	V_{oc} (V)	FF	PCE (%)
PSBTBT:mono-PCBM = 1:2 (film thickness 190 nm)	5.23	0.55	0.21	0.64
PCPDTBT:mono-PCBM = 1:3.4 (film thickness 169 nm)	5.29	0.67	0.39	1.48

it is likely to be related to a non-optimal carrier extraction at one of the two interfaces, rather than being a property of the bulk. The effect was not observed in the case of doctor-bladed films[14,15] and may therefore be related to the specific coating conditions of the inkjet printing. The presence of the kink only in the case of the PSBTBT-based devices suggests that its origin is in relation to the lower solubility of the silicon-bridged polymer.

Despite the low photocurrent and fill factor for both systems, the best obtained power efficiency was 0.64% and 1.48% for the PSBTBT:mono-PCBM and PCPDTBT:mono-PCBM, respectively. These values are relatively high when taking into account that the printing was far from ideal; the active layers were inkjet printed at room temperature and under normal lab conditions, *i.e.* non-optimized and no clean room conditions. Therefore, dust particles may have been introduced in the process. Printing the active layers under clean room conditions would increase the efficiencies.

3. Conclusions

In this contribution, the screening of different polymer:fullerene blends in a combinatorial manner was achieved by using inkjet printing techniques. The experimental workflow presented here allowed a fast and simple evaluation of potential donor/acceptor combinations for the use in organic photovoltaics. Inkjet printing required less material and showed a higher reproducibility. Furthermore, inkjet printing produces low amounts of waste, yielding high material efficiencies in contrast to spin-coating.

Two polymers (PCPDTBT, PSBTBT) and two fullerenes (mono-PCBM, bis-PCBM) were used to prepare different blend compositions. It was found that for the polymer:fullerene blends a solvent system of chlorobenzene/*ortho*-dichlorobenzene (CB/*o*-DCB) with a ratio of 90/10 and a plasma surface pre-treatment were necessary to obtain homogeneous films. In order to obtain films with a thickness between 100 and 200 nm, a concentration of 0.5 wt% was used.

Morphological investigations by AFM revealed a good intermixing of the polymer and fullerene components. Smooth, thin films were obtained with the polymer PCPDTBT, whereas the polymer PSBTBT showed aggregate formation, which may be due to the reduced solubility of the PSBTBT polymer in the solvent system used. Screening the optical properties of the inkjet printed films showed an efficient quenching of polymer emission that is characteristic for an efficient charge transfer and a good intermixing of the blend compounds. From this combinatorial study, two blends were tested for their solar cell activity. A maximum power conversion efficiency of 0.64% and 1.48% was obtained for the PSBTBT:mono-PCBM and PCPDTBT:mono-PCBM systems, respectively.

It was observed that small changes in the chemical structure of the polymer (C-bridged *vs.* Si-bridged) lead to significant changes in film formation properties. As a result, each polymer:fullerene blend requires a unique investigation to obtain optimal properties for the usage in organic solar cells. The experimental setup and the combinatorial study presented here enables a fast and efficient screening of the polymer:fullerene blends. When using inkjet printed thin-film libraries, small amounts of material are necessary to investigate structure-property relationships between the active compounds and their efficiency in organic solar cells.

Furthermore, the solar cells results clearly highlight the potential of the inkjet method for the preparation of large area organic photovoltaics (OPV), but also point out the necessity of this coating technology to further evolve in complexity, in order to provide the level of control over the specific coating parameter space, required by OPV.

4. Experimental Section

Materials: The polymers PCPDTBT (M_n = 21,000 g mol^{-1}, PDI ~ 2.4) and PSBTBT (M_n = 23,000 g mol^{-1}, PDI ~ 2.1) were obtained from Konarka as powders. The fullerene derivatives mono-PCBM and bis-PCBM were obtained from Solenne (99% pure). The solvents chlorobenzene (CB) and *ortho*-dichlorobenzene (*o*-DCB) were purchased from Aldrich (Steinheim, Germany) and filtered before usage. Stock solutions from each compound were prepared by dissolving in CB while stirring and heating at 70 to 90 °C overnight. The inks with a systematically varied polymer:fullerene ratio and varied chlorobenzene/*ortho*-dichlorobenzene (CB/*o*- DCB) ratio were prepared utilizing a pipetting robot (FasTrans, Analytik Jena, Jena, Germany).

Preparation of substrates: Microscope slides (75 × 25 mm^2) from Marienfeld (Lauda-Königshofen, Germany) were used as glass substrates. The substrates were rinsed with *iso*-propanol and dried with an airflow. An oxygen plasma treatment for two minutes at 150 W (Diener Electronic, Nagold, Germany) was performed to remove any remaining organic compounds and to improve the wetting behavior of the glass substrates.

Instrumentation: The printing experiments were carried out with an Autodrop system from microdrop Technologies (Norderstedt, Germany). The printer was equipped with a piezo-based printhead (micropipette system AD-K-501) with an inner diameter of 70 µm and a storage volume of 25 µL. As reservoir, a 96-well quartz microtiter plate was used. The solutions were aspirated from a single well and then dispensed onto the substrate as films of 5 × 5 mm^2. Voltages between 65 and 70 V and pulse lengths between 30 and 35 µs were found to create stable droplets. Inkjet printing from a heated solution was performed with a heatable dispenser (AD-K-801) operating at a voltage of 105 V and a pulse length of 45 µs. Standard settings for the printing speed (10 mm s^{-1}) and the drop count (five drops) were used.

Spin-coating was performed at a spin speed of 1,600 rpm and an acceleration of 1,080 rpm s^{-1} with a spin-coater from Laurell Technologies Corporation (North Wales, USA). The spin-coating time was set to 30 seconds.

Surface topography and film thickness measurements were performed with an optical interferometric profiler Wyko NT9100 (Veeco, Mannheim, Germany). In each film a scratch was made using a scalpel. The depth of the scratch was measured at five different positions in the resulting line and the values were averaged.

A UV-vis absorption/fluorescence plate reader from Analytik Jena (FLASHScan 530, Jena, Germany) was used to measure the UV-vis absorption spectra of the printed films.

Atomic force microscopy (AFM) measurements were performed in tapping mode with an NTegra Aura (NT-MDT, Moscow, Russia) and a Nanoscope IIIa Multimode (Digital Instruments, Veeco, Mannheim, Germany) with commercially available cantilevers. TiN coated AFM tips (m-Mash, Estonia) were used, which reduce the adhesion to the films significantly. The scan area was either 2×2 μm^2 or 2.5×2.5 μm^2. All measurements were performed in the center of the respective sample.

Preparation of polymer solar cells: Bulk heterojunction devices were produced on indium tin oxide (ITO) coated glass substrates that were used as transparent bottom electrode. A layer of poly(ethylene dioxythiophene) doped with polystyrene sulfonic acid (PEDOT:PSS, Clevios) was coated on top of the ITO with a layer thickness of 70 nm. The organic semiconductor blend, consisting either of a blend ratio 1:3.4 of PCPDTBT and mono-PCBM or of a blend ratio 1:2 of PSBTBT and mono-PCBM, was inkjet printed from CB/*o*-CDB (ratio 90/10) on top of the PEDOT layer. LiF/Al was deposited as a top electrode material by thermal evaporation. The active area is approximately 10 mm^2. Annealing of the devices was performed at 90°C for 10 minutes.

Instrumentation for measuring solar cell performance: The photoluminescence of the films was recorded at room temperature and ambient atmosphere by employing a 325 nm He:Cd laser with an excitation power density of approximately 0.4 W cm^{-1}. A monochromator with a focal length of 550 mm, a grating with 100 grooves per mm, and a liquid-nitrogen-cooled CCD with 1024×512 pixels were used for luminescence analysis.

The current-density-voltage characteristics of the devices were measured under nitrogen atmosphere and AM1.5 illumination (0.1 W cm^{-2}) using a source measurement unit SMU 2400 from Keithley.

Supporting Information

Supporting Information is available from the Wiley Online Library or from the author.

Acknowledgements

The authors would like to thank Konarka and the DPI (technology area HTE) for financial support.

Received: September 26, 2010
Revised: November 14, 2010
Published online: December 15, 2010

[1] A. C. Grimsdale, K. L. Chan, R. E. Martin, P. G. Jokisz, A. B. Holmes, *Chem. Rev.* **2009**, *109*, 897.
[2] J. H. Burroughes, D. D. C. Bradley, A. R. Brown, R. N. Marks, K. Mackay, R. H. Friend, P. L. Burns, A. B. Holmes, *Nature* **1990**, *347*, 539.
[3] A. Menon, H. P. Dong, Z. I. Niazimbetova, L. J. Rothberg, M. E. Galvin, *Chem. Mat.* **2002**, *14*, 3668.
[4] S. Günes, H. Neugebauer, N. S. Sariciftci, *Chem. Rev.* **2007**, *107*, 1324.
[5] C. J. Brabec, N. S. Sariciftci, J. C. Hummelen, *Adv. Funct. Mater.* **2001**, *11*, 15.
[6] T. Kawase, T. Shimoda, C. Newsome, H. Sirringhaus, R. H. Friend, *Thin Solid Films* **2003**, *438*, 279.
[7] H. N. Tsao, D. Cho, J. W. Andreasen, A. Rouhanipour, D. W. Breiby, W. Pisula, K. Müllen, *Adv. Mater.* **2009**, *21*, 209.
[8] H. Hoppe, N. S. Sariciftci, *J. Mater. Res.* **2004**, *19*, 1924.
[9] E. Tekin, D. A. M. Egbe, J. M. Kranenburg, C. Ulbricht, S. Rathgeber, E. Birckner, N. Rehmann, K. Meerholz, U. S. Schubert, *Chem. Mat.* **2008**, *20*, 2727.
[10] B. J. de Gans, P. C. Duineveld, U. S. Schubert, *Adv. Mater.* **2004**, *16*, 203.
[11] J. C. Bijleveld, M. Shahid, J. Gilot, M. M. Wienk, R. A. J. Janssen, *Adv. Funct. Mater.* **2009**, *19*, 3262.
[12] M. Morana, H. Azimi, G. Dennler, H. J. Egelhaaf, M. Scharber, K. Forberich, J. Hauch, R. Gaudiana, D. Waller, Z. H. Zhu, K. Hingerl, S. S. van Bavel, J. Loos, C. J. Brabec, *Adv. Funct. Mater.* **2010**, *20*, 1180.
[13] H. Y. Chen, J. H. Hou, A. E. Hayden, H. Yang, K. N. Houk, Y. Yang, *Adv. Mater.* **2010**, *22*, 371.
[14] M. C. Scharber, M. Koppe, J. Gao, F. Cordella, M. A. Loi, P. Denk, M. Morana, H. J. Egelhaaf, K. Forberich, G. Dennler, R. Gaudiana, D. Waller, Z. G. Zhu, X. B. Shi, C. J. Brabec, *Adv. Mater.* **2010**, *22*, 367.
[15] D. Mühlbacher, M. Scharber, M. Morana, Z. G. Zhu, D. Waller, R. Gaudiana, C. Brabec, *Adv. Mater.* **2006**, *18*, 2884.
[16] J. K. Lee, W. L. Ma, C. J. Brabec, J. Yuen, J. S. Moon, J. Y. Kim, K. Lee, G. C. Bazan, A. J. Heeger, *J. Am. Chem. Soc.* **2008**, *130*, 3619.
[17] M. Lenes, G. J. A. H. Wetzelaer, F. B. Kooistra, S. C. Veenstra, J. C. Hummelen, P. W. M. Blom, *Adv. Mater.* **2008**, *20*, 2116.
[18] F. C. Krebs, *Sol. Energy Mater. Sol. Cells* **2009**, *93*, 394.
[19] E. Tekin, P. J. Smith, U. S. Schubert, *Soft Matter* **2008**, *4*, 703.
[20] M. Singh, H. M. Haverinen, P. Dhagat, G. E. Jabbour, *Adv. Mater.* **2010**, *22*, 673.
[21] C. N. Hoth, S. A. Choulis, P. Schilinsky, C. J. Brabec, *Adv. Mater.* **2007**, *19*, 3973.
[22] C. N. Hoth, S. A. Choulis, P. Schilinsky, C. J. Brabec, *J. Mater. Chem.* **2009**, *19*, 5398.
[23] C. N. Hoth, P. Schilinsky, S. A. Choulis, C. J. Brabec, *Nano Lett.* **2008**, *8*, 2806.
[24] B. J. de Gans, E. Kazancioglu, W. Meyer, U. S. Schubert, *Macromol. Rapid Commun.* **2004**, *25*, 292.
[25] B. J. de Gans, U. S. Schubert, *Macromol. Rapid Commun.* **2003**, *24*, 659.
[26] E. Tekin, B. J. de Gans, U. S. Schubert, *J. Mater. Chem.* **2004**, *14*, 2627.
[27] E. Tekin, H. Wijlaars, E. Holder, D. A. M. Egbe, U. S. Schubert, *J. Mater. Chem.* **2006**, *16*, 4294.
[28] H. Hoppe, N. S. Sariciftci, *J. Mater. Chem.* **2006**, *16*, 45.
[29] M. Morana, M. Wegscheider, A. Bonanni, N. Kopidakis, S. Shaheen, M. Scharber, Z. Zhu, D. Waller, R. Gaudiana, C. Brabec, *Adv. Funct. Mater.* **2008**, *18*, 1757.
[30] X. Yang, J. Loos, *Macromolecules* **2007**, *40*, 1353.
[31] J. Jo, S. S. Kim, S. I. Na, B. K. Yu, D. Y. Kim, *Adv. Funct. Mater.* **2009**, *19*, 866.
[32] G. Li, V. Shrotriya, Y. Yao, J. S. Huang, Y. Yang, *J. Mater. Chem.* **2007**, *17*, 3126.
[33] E. Tekin, E. Holder, V. Marin, B. J. de Gans, U. S. Schubert, *Macromol. Rapid Commun.* **2005**, *26*, 293.
[34] V. Marin, E. Holder, M. M. Wienk, E. Tekin, D. Kozodaev, U. S. Schubert, *Macromol. Rapid Commun.* **2005**, *26*, 319.
[35] R. D. Deegan, O. Bakajin, T. F. Dupont, G. Huber, S. R. Nagel, T. A. Witten, *Phys. Rev. E* **2000**, *62*, 756.
[36] X. Y. Shen, C. M. Ho, T. S. Wong, *J. Phys. Chem. B* **2010**, *114*, 5269.